LA-UR -84-2054

Los Alamos National Laboratory is operated by the University of California for the United States Department of Energy under contract W-7405-ENG-36

CONF-8409104--2

LA-UR--84-2054

DE84 014010

TITLE: RESERVOIR SIZING USING INERT AND CHEMICALLY REACTING TRACERS

AUTHOR(S): Bruce A. Robinson (Massachusetts Institute of Technology; ESS-4)

Jefferson W. Tester (Massachusetts Institute of Technology)

Lee F. Brown (ESS-5)

SUBMITTED TO: 59th Annual Conference & Exhibition
Society of Petroleum Engineers
Houston, TX, September 16-19, 1984

DISCLAIMER

Los Alamos Los Alamos National Laboratory
Los Alamos, New Mexico 87545

FORM NO 836 R4
ST NO 2629 5/81

DISCLAIMER

RESERVOIR SIZING USING INERT AND CHEMICALLY REACTING TRACERS

Bruce A. Robinson and Jefferson W. Tester
Department of Chemical Engineering, Massachusetts Institute of Technology
Cambridge, MA 02139

and

Lee F. Brown
Earth and Space Sciences Division, Los Alamos National Laboratory
Los Alamos, NM 87545

ABSTRACT

Non-reactive tracer tests in prototype hot dry rock (HDR) geothermal reservoirs indicate multiple fracture flow paths that show increases in volume due to energy extraction. Tracer modal volumes correlate roughly with estimated reservoir heat-transfer capacity. Chemically reactive tracers are proposed which will map the rate of advance of the cooled region of an HDR reservoir, providing advanced warning of thermal drawdown. Critical parameters are examined using a simplified reservoir model for screening purposes. Hydrolysis reactions are a promising class of reactions for this purpose.

INTRODUCTION

Tracers have become a useful and reliable diagnostic tool for determining the size and fluid flow characteristics of geothermal reservoirs.[1-3] The fundamental premise underlying their use is that the tracer follows the same flow paths with the same flow fractions as the injected reservoir fluid itself. When this principle is applied to steady state flow in a fractured hot dry rock (HDR) geothermal reservoir, fracture volumes and degree of dispersion take on precise meaning.[1]

The first section of this paper is an overview of the results obtained from inert tracer experiments performed in the HDR geothermal reservoirs operated at Fenton Hill, NM and at the Rosemanowes Quarry in Cornwall, U.K. Here we focus on model-independent information such as fracture volumes and dispersive characteristics, and derive general conclusions about the behavior of fractured geothermal reservoirs. Since the information supplied by conventional reservoir tests is probably insufficient to construct reliable reservoir models with predictive capabilities, we are developing the new technique of injection of temperature-sensitive chemically reacting tracers. These tracers will directly measure the rate of cooldown of the rock between the two wellbores of a continuous flow geothermal reservoir. These tests should also be

References and Illustrations at end of paper.

useful in conventional geothermal reservoirs in which reinjection creates the undesirable side effect of produced fluid thermal drawdown. The second section of this paper explores the strengths and limitations of the reactive tracer concept using a simple one-dimensional dispersion model for illustrative purposes. The final section is an update on our ongoing laboratory kinetic studies aimed at identifying reactive tracers suitable for different reservoir conditions.

INERT TRACER ANALYSIS

Definitions

1. Residence Time Distribution, E(t): E(t)dt = the fraction of the injected fluid which exits the system between t and t + dt. For tracers which follow the same flow paths as the reservoir fluid, the concentration-time response measured at the outlet to a pulse injected at the inlet is:

$$C(t) = \frac{m_p E(t)}{Q} \qquad (1)$$

where m_p is the mass of tracer injected, and Q is the volumetric flow rate of fluid. In this paper, we will often refer to the residence time distribution (RTD) curve as E(V), where E(V) = E(t)/Q. This convention allows us to compare directly fracture volumes measured in tracer experiments at different flow rates.

2. Modal Volume, $\dot{V}$: the volume corresponding to the peak of the RTD curve. In flow through fractured geothermal reservoirs, $\dot{V}$ most likely represents the volume of low impedance connections ($\Delta P/Q$ is small) which follow a direct route from inlet to outlet.

3. Integral Mean Volume, <V>:

$$\langle V \rangle = \int_0^\infty VE(V)dV \qquad (2)$$

In fractured porous media, <V> is the void volume of all fractures which accept flow, regardless of their impedance. Since measurement of the tail of

a distribution is inaccurate and the curve must be arbitrarily extended to infinite volume, the calculated integral mean volume should be considered an approximate estimate of the entire fracture system volume.

4. Width at 1/2 Height, $w_{1/2}$: the width between the two points on either side of the peak for which the tracer response is one-half its peak value. This parameter, though defined arbitrarily, is a measure of the outlet dispersion of the main fracture flow paths. By using only the front part of the distribution, this approach circumvents the problem of the inaccurate tail which decreases the usefulness of the variance as a measure of dispersion.

5. Effective Heat Transfer Surface Area, A: a single-parameter estimate of the heat transfer capacity of a fractured reservoir. Assuming plug flow up a single vertical, rectangular fracture of surface area A (on one face of the fracture), the fluid temperature within the fracture during long-term operation is given by:[4]

$$\frac{T-T_i}{T_r-T_i} = \text{erf}\left[\frac{\lambda_r A(z/L)}{\rho c_p Q\sqrt{\alpha t_{op}}}\right] \qquad (3)$$

where T, T_i, and T_r are the fluid, inlet, and initial temperatures, λ_r and α the thermal conductivity and thermal diffusivity of the rock, ρ and c_p the average density and heat capacity of the fluid, and t_{op} the time of operation of the reservoir. The outlet fluid temperature is obtained by setting $z/L = 1$. Although simplistic, this model conveniently describes the long-term behavior of a fractured reservoir with a single adjustable parameter.

Dispersion Mechanisms

The outlet tracer response from a fractured geothermal reservoir is a combination of two effects: (1) large scale flow heterogeneities such as fractures of different size and flow impedance, and (2) dispersion resulting from flow through a single fracture. The large scale heterogeneities will undoubtedly exert greater influence on the heat transfer behavior, since the positioning of low impedance conduits effectively defines the accessible volume of rock in a fractured reservoir. Indeed, the onset and subsequent rate of thermal drawdown is probably controlled by the surface area of the smallest low impedance connection. However, proper interpretation of a tracer-determined RTD curve requires an evaluation of the magnitude of dispersion within a single fracture.

Horne and Rodriguez[5] and Robinson and Tester[1] evaluated various single-fracture dispersion mechanisms for conditions likely in fractured geothermal reservoirs. Table 1 summarizes the results of these studies, using the axial dispersion Peclet number ($Pe = UL/D_{eff}$) as the parameter characterizing dispersion. A large Peclet number indicates that the mechanism produces very little of the observed outlet dispersion. The main conclusion from these studies is that the amount of

dispersion produced within a single fracture is small compared with the overall level of dispersion measured in HDR reservoirs using tracers. Multi-fractured reservoirs appear to be the rule for the systems tested at Fenton Hill.

This conclusion was corroborated in the radioactive ^{82}Br tracer experiments at Fenton Hill using gamma logging in the production wellbore. Distinct concentration-time curves were identified for three exit regions in the production wellbore. In a series of tracer tests, we were able to identify marked changes in the internal flow field of the reservoir.[1]

Empirical Correlations

Despite the existence of detailed flow information from tracers, flow impedance measurements, and downhole logging, no unique reservoir model was constructed for the latest Fenton Hill reservoir.[6] Tracers are useful for measuring fracture volume and flow fractions, but cannot be used easily to determine the distribution and orientation of fractures in space. In future reservoirs, more sophisticated injection schemes could be used to improve the technique, such as preferential tracer injection into a single fracture, followed by monitoring different production regions by gamma logging. However, in analyzing past tracer experiments in the Fenton Hill and Rosemanowes reservoirs,[7] we have found an empirical approach to be as useful as deterministic reservoir simulations. We may draw correlations from a series of tracer experiments in the same reservoir, or from tests in different reservoirs. These correlations lead to general conclusions about the nature of flow and heat transfer in fractured geothermal reservoirs.

For flow through a single fracture or several fractures, the tracer dispersion measured by $w_{1/2}$ appears to scale directly with fracture volume. The ratio $w_{1/2}/\dot{V}$ in Table 2 varies over a quite narrow range, considering that these systems span three orders of magnitude in size. These reservoirs exhibit similar dispersive characteristics in their main fracture flow paths, each being the result of flow through several (at least 3-5) fractures.

The modal volume $\dot{V}$ corresponds to the low impedance fracture connections, which should contribute most to the long term produced fluid temperature decline. As seen in Figure 1, $\dot{V}$ correlates with the reservoir's heat transfer capacity. The effective heat transfer surface area A was calculated by applying Eqn. (3) (or, in some cases, a slightly modified version of this expression) to actual produced fluid thermal drawdown data for each reservoir. A single tracer experiment provides a rough estimate of the heat extraction capability of a fractured reservoir. The Rosemanowes Phase II point in Figure 1 is not a data point, as extensive energy extraction has not been carried out in this reservoir. We include it to show that for this new reservoir and commercial-sized systems, use of the overall modal volume to estimate A is unjustified because of the large extrapolation from present day experience. A more legitimate approach in systems with multiple

entrance and exit regions would be to size individual fracture zones using preferential injection of a radioactive tracer and production well gamma logging.[8] These subsystems are likely to be small enough to warrant the use of Figure 1.

This simple analysis ignores the fact that not all fluid travels directly from entrance to exit in low impedance fractures. The Run Segment 5 tracer experiments at Fenton Hill (5/9/80 to 12/12/80) showed that in this reservoir roughly 30% of the injected fluid traveled through high impedance secondary joints.[1] This result appears to be quite common in the HDR reservoirs tested to date: flow through several low impedance joints accounts for the early tracer response, while a substantial secondary flow travels through a large volume of rock at the periphery of the reservoir. The integral mean volume [Eqn. (2)] is the total fracture volume (main fractures plus secondary flow paths). As seen in Table 2, the integral mean volumes for the ^{82}Br tracer experiments of Run Segment 5 are much larger than the corresponding modal volumes. The enormous potential capacity of this reservoir probably went largely unused due to the tendency of the fluid to short-circuit in low impedance joints. Total reservoir size estimates using microseismic mapping and geochemical information also substantiate this conclusion.[9]

In addition to absolute size, reservoir growth during energy extraction may be monitored in a series of tracer tests using $\dot{V}$ and $\langle V \rangle$. Fracture volume growth may be caused by either thermal contraction and stress cracking of rock during cooldown, or the opening of new fractures by water permeation into pre-existing joints in the rock matrix (hydraulic fracturing). The increase in modal and integral mean volumes during Run Segment 5 are plotted against total energy extracted in Figure 2. The maximum amount of new fracture volume possible via thermal contraction of rock is denoted by the free thermal expansion line. The large increase in integral mean volume suggests that hydraulic fracturing must have been occurring along with thermal contraction. However, much of this new volume was poorly utilized, as evidenced by the modest increase in modal volume.

For reservoirs operated with steady flow conditions, the need for low impedance fracture connections may be at odds with the goal of achieving a volumetric sweep of fluid through a large number of fractures. Different operating strategies in future HDR reservoirs may allow us to utilize more efficiently the large fracture volumes which apparently possess only a relatively weak hydraulic connectivity with the main fractures. Rapid pressurization of a partially cooled reservoir could result in a more evenly distributed flow through a larger number of fractures. Experimental proof of this contention is seen in the dramatic increase in modal volume caused by rapid pressurization in the stress unlocking experiment (SUE) on 12/8/80. A series of these high pressure experiments, or possibly cyclical pressure transients, could bring more of the unused far-field fracture volume into the active heat exchange region of a fractured reservoir. Alternatively, huff-puff operation -- injection into a shut-in reservoir, followed by production from the same well -- might provide greater access to a larger

volume of hot rock. Because tracer experiments measure fracture volume, they will be invaluable in evaluating the success of these proposed techniques.

RESERVOIR ANALYSIS USING REACTING TRACERS

Analysis of small, prototype reservoirs was made manageable by the ability to achieve produced fluid temperature decline after only a few months of operation. However, for larger systems, reservoir simulators will have to be used in a predictive way, since thermal drawdown measurements could take years to produce useful modeling information. More importantly, commercialization of the HDR concept requires that a method exist for predicting a priori the lifetime of a reservoir. The normal battery of diagnostic experiments (pressure transient, well logging, tracer, microseismic, and fluid geochemical) probably does not provide the information necessary to construct detailed reservoir models with predictive capability. Chemically reactive tracers, which are sensitive to internal changes to the reservoir's temperature field, may solve this problem in future HDR systems.

The kinetics of most chemical reactions are extremely temperature-sensitive. For first order reactions carried out in batch reactors, the following rate equation is often applicable:

$$\frac{dC}{dt} = -kC \quad , \tag{4}$$

where C is the concentration of the reacting species and t is time. The rate constant k is the parameter which contains the temperature sensitivity. It normally can be described by the equation

$$k = A_r e^{-E_a/RT} \quad , \tag{5}$$

where A_r is the pre-exponential factor, E_a the activation energy of the reaction, R the universal gas constant, and T the absolute temperature. For typical reactions in solution, k will vary by several orders of magnitude for the range of temperatures encountered in an HDR reservoir undergoing extensive energy extraction.

Suppose a tracer is injected into an initially hot reservoir, and the reaction proceeds about half way to completion during its stay in the system. Then, after some cooldown has been achieved, a second experiment should show less chemical reaction because of the shorter time the fluid spends in hot rock. A series of reactive tracer experiments will, in theory, map the rate of progress of the cooled region as it approaches the exit well, giving an early warning of thermal drawdown.

The transient response of this reacting tracer experiment will be governed by both the temperature field and the dispersive nature of the fluid flow. For preliminary estimates, we assumed that the tracer behavior could be modeled using the one-dimensional axial dispersion equation with a first-order chemical reaction included:

$$\frac{\partial C}{\partial t} = D_{eff}\left(\frac{\partial^2 C}{\partial z^2}\right) - U\left(\frac{\partial C}{\partial z}\right) - kC \qquad (6)$$

Although objections have been raised against the applicability of Eqn. (6) for fractured porous media, we use it here to demonstrate the concept of reactive tracers and to perform parameter sensitivity studies. Since chemical reaction rates for first order reactions depend on the time-temperature history of the fluid rather than on the specific dispersion mechanism, Eqn. (6) should be adequate for these scoping calculations.

The other component of this reservoir model is to superimpose an axial (z-direction) temperature field on the flow field. The single-fracture temperature solution [Eqn. (3)] will be used in these calculations. This uniform temperature field assumption is perhaps the weakest aspect of the model, given the explanation of tracer dispersion as flow through different sized fractures. These fractures are each likely to have unique temperature characteristics, the small ones (corresponding to short residence times) cooling down more rapidly than the large ones. Nonetheless, the model as formulated should be sufficient for parameter studies. Analysis of actual experiments will probably have to account for the objection just raised.

The most important feature of the reactive tracer concept is its ability to identify thermal drawdown much more quickly than simple produced-fluid temperature measurements. For $A = 300000\ m^2$, $Q = 1.262 \cdot 10^{-2}\ m^3/s$ (200 gpm), and $T_{init} = 250°C$, the internal temperature field in a reservoir at various times is shown in Figure 3. To achieve 10°C of produced fluid thermal drawdown (the bare minimum for estimating reservoir size), five years of continuous operation are required. The reactive tracer response to a step change in inlet concentration is shown in Figure 4. Just 1-2 years of operation are required to obtain a sensitive estimate of heat exchange capacity.

Parameter studies using the axial dispersion model also support the following conclusions:

- For thermal behavior like that in Figure 3, reactions with higher activation energy are more sensitive to small levels of thermal drawdown. For the example shown above, $E_a = 90$ kJ/mol and the measurement required 1-2 years of operation to be successful. This requirement would be closer to two years for $E_a = 43$ kJ/mol, but only one year for $E_a = 130$ kJ/mol.

- Tracer dispersion affects the shape of the response curves, but not the sensitivity of the measurement. However, notice that the response curves of Figure 4 are compared with the non-reacting tracer response curve. A reactive tracer experiment should always be accompanied with an inert tracer test run simultaneously, especially since the inert tracer response curves tend to shift markedly toward longer residence times (because of reservoir growth) during long term operation.

• The reactive tracer response is sensitive to the extent of thermal drawdown, but not to the specific shape of the temperature field. Reactions which are moderately fast at the highest reservoir temperature are extremely slow at temperatures 100°C below this. Thus, the exact shape of the temperature field in the cooled region of the reservoir is unimportant. The conversion of a reacting tracer is essentially a measure of the amount of hot rock remaining between the two wellbores. The term "hot" is dependent somewhat on the activation energy of the reaction, as was discussed above.

• The shape of the transient reactive tracer response curve is significantly different than those in Figure 4 for nonuniform temperature fields. The model used in Figures 3 and 4 assumed a single temperature field for all flow paths, regardless of residence time. A plausible alternative in fractured geothermal reservoirs is the model of Nichol and White,[10] which posits that short residence times correspond to fractures of smaller surface area which cool more rapidly than those of longer residence time. If a pulse of reactive tracer were injected, the response from a nonuniform temperature field would exhibit a higher peak than that from the uniform temperature field, and then would descend more steeply to a region below the uniform-temperature-field response. This sort of comparison between models and actual experimental data should help in the construction of complex simulations of future reservoirs. The analysis should provide information on not only reservoir capacity, but also the distribution of fracture surface areas.

REACTIVE TRACER KINETIC STUDIES

In addition to the modeling work described above, we are performing laboratory kinetic experiments to find suitable reactive tracers for different reservoir conditions. The reaction rate parameters (A_r and E_a) must be such that the reaction time at the initial reservoir temperature is on the order of the average fluid residence time in the reservoir. Reactions with easily characterized rate behavior are preferable to those exhibiting complex kinetic properties. Also, adsorption of reactants and products on the reservoir rock surfaces should be negligible. Finally, the chemical analysis of reactants and products must be sensitive enough to detect low concentrations accurately. Otherwise, an unreasonably large quantity of tracer would have to be injected.

We are currently studying the alkaline hydrolysis of organic esters and amides in water for use as chemically reactive tracers:

$$\text{Esters:}\quad RCOOR' + OH^- \rightleftharpoons RCOO^- + R'OH \qquad (7)$$

$$\text{Amides:}\quad RCONH_2 + OH^- \rightleftharpoons RCOO^- + NH_3 \qquad (8)$$

Under typical geochemical conditions, many esters and amides obey the following rate law:

$$\frac{dC}{dt} = -k_2[OH^-]C \qquad (9)$$

where C is the concentration of the ester or amide, and k_2 the second order rate constant (with units liters/mol-s), and $[OH^-]$ the

hydroxide ion concentration. The product $k_2[OH^-]$ is a pseudo-first order rate constant which plays the role of k in the first order rate expression [Eqn. (4)]. To fully understand the first order alkaline hydrolysis mechanism, we must model the terms k_2 and $[OH^-]$ separately.

In concentrated NaOH solutions at room temperature, $[OH^-]$ is simply calculated by $[OH^-] = 10^{(pH-14)}$. However, the OH^- concentration in a typical geofluid at high temperature is much different from the value measured by pH at room temperature because of the increase in the ionization constant of water with temperature. This situation is modeled approximately assuming the following liquid phase equilibrium reactions:

$$H_2O \rightleftarrows H^+ + OH^-; \qquad K = [H^+][OH^-] \qquad (10)$$

$$H_2CO_3 \rightleftarrows H^+ + HCO_3^-; \qquad K = \frac{[H^+][HCO_3^-]}{[H_2CO_3]} \qquad (11)$$

The equilibrium constants K for these reactions follow the van't Hoff relation:

$$\ln\left(\frac{K_T}{K_{25}}\right) = \frac{\Delta H^o}{R}\left(\frac{1}{298.2} - \frac{1}{T}\right) \qquad (12)$$

The heats of reaction ΔH^o for Reactions (10) and (11) are 57.4 and 11.6 kJ/mol, respectively.

Our goal is to calculate $[OH^-]$ as a function of temperature, given measurements of $[H^+]$ and $[HCO_3^-]$ for the fluid sample at 25°C. If $[H^+]$ and $[HCO_3^-]$ are measured at room temperature, then equilibrium-constant expressions allow us to calculate the concentrations of all species in Eqns. (10) and (11) at 25°C. Concentrations at high temperature are then obtained by calculating the new equilibrium constants using Eqn. (12), using the concentrations at 25°C as initial conditions, and assuming the reactions proceed stoichiometrically to the new equilibrium position at the upper temperature.

Figure 5 shows the behavior of $[OH^-]$ with temperature for the case of pH = 6.0 and $[HCO_3^-]$ = 1000 ppm, both at 25°C. The hydroxide concentration increases dramatically with temperature due to the water dissociation reaction. Other calculations show that in the pH range of 5-7, similar straight line $\log [OH^-]$ versus 1/T behavior should be observed as long as bicarbonate ion is present in quantities of over roughly 100 ppm. Thus, $[OH^-]$ may be conveniently calculated by

$$\ln \frac{[OH^-]_T}{[OH^-]_{25}} = \frac{45.8}{R}\left(\frac{1}{298.2} - \frac{1}{T}\right) \qquad (13)$$

Notice that 45.8 kJ/mol is the difference in the heats of reaction of the two ionization reactions.

Eqn. (13) implies a $\ln [OH^-]$ versus 1/T straight line behavior. The second order rate constant k_2 also possesses this type of temperature dependence. Therefore, the pseudo-first order rate

constant $k = k_2[OH^-]$ will exhibit an Arrhenius behavior. Combining Eqn. (13) with the Arrhenius equation for k_2, we obtain for the first order rate constant parameter expressions:

$$A_r = 10^{pH}(1.0457 \cdot 10^{-6})A_{r,2} \qquad (14)$$

$$E_a = 45.8 + E_{a,2} \qquad (15)$$

where the subscript 2 refers to the second order rate constant k_2.

Experimental kinetic studies have been performed so far on five organic esters and one amide to obtain the second order rate constant k_2 as a function of temperature, and also to verify the model for $[OH^-]$ just presented. Mixtures of sodium bicarbonate and acetic acid were used as a buffer system. By keeping the $NaHCO_3$ concentration at 2750 ppm and varying the amount of acetic acid added, we were able to adjust the pH at room temperature in the range of interest. In this simulated brine, the acetic acid ionization reaction also had to be included in the calculation, but the behavior of $[OH^-]$ versus T was nonetheless quite similar to that described above. In addition to the advantage of pH adjustability, the acetic acid buffered the solution to the point where the production of carboxylic acids via the hydrolysis reaction had virtually no effect on the pH.

The hydroxide concentration model was tested experimentally in two ways. First, several experiments at different temperatures but the same starting pH were performed. Second order rate constants were back-calculated using the first order rate expression and the equilibrium model for $[OH^-]$. These results are presented in Table 3 in the form of second order Arrhenius parameters. These parameters agree well with kinetic results tabulated by Kirby,[11] despite the fact that previous studies were performed in the temperature range from 30-60°C and NaOH concentration on the order of 1 M. Without the $[OH^-]$ model, our rate data are inexplicable. For instance, if kinetic parameters are calculated by naively assuming $[OH^-] = 10^{(pH-14)}$, without accounting for the increase of ionization of water with temperature, the values of k_2 are 2-3 orders of magnitude too high, and the activation energies are much larger than those given by Kirby.[11] The second check on the model was to run experiments at the same temperature and different pH. This comparison yielded the correct rate versus pH behavior as predicted by the model. We feel that these results are powerful evidence of the validity of the hydroxide concentration model for the compounds listed in Table 3.

One other ester which was tested but not listed in the table is tert-butyl acetate. Its rate was much more rapid than expected from previous studies, and it did not exhibit the rate-pH behavior predicted by the model. The reaction mechanism is clearly different for tert-butyl acetate under these conditions, a fact which may be explained by Kirby's observation that the hydrolysis of esters of tertiary alcohols are acid catalyzed even at low acid concentrations.[11]

The kinetic data obtained so far are plotted in a convenient form in Figure 6. The reaction time $\tau_R = 1/(k_2[OH^-])$ is the time required for the reactant concentration to proceed to 1/e of its original value. To choose the appropriate tracer, τ_R should roughly equal the typical fluid residence time in the reservoir. For various reservoir temperatures, pH's, and residence times, plots such as Figure 6 may be used to choose an appropriate reactive tracer. As shown in the figure, tracers have been identified for cool systems (80-100 °C) and reservoirs of moderate temperature (170-200 °C). In future kinetic experiments, we intend to fill the gap which exists between these two groups, and also identify tracers for much hotter reservoirs.

CONCLUSIONS

1. Levels of dispersion in tracer field experiments of HDR reservoirs indicate that the majority of flow is through a number of low impedance fractures. However, up to 30% of the flow travels through high impedance secondary flow paths of large volume.

2. Reservoir heat transfer capacity measured by effective heat transfer surface area A correlates with tracer modal volume $\hat{V}$.

3. Tracer dispersion scales approximately linearly with reservoir modal volume.

4. The volume of secondary flow paths grows substantially during long term energy extraction. More uniform flow and hence better utilization of high impedance joints was achieved by rapid pressurization of the Fenton Hill reservoir during the stress unlocking experiment.

5. Preliminary modeling suggests that the injection of chemically reactive tracers should be a sensitive reservoir test for measuring thermal drawdown far in advance of actual produced fluid temperature decline.

6. Laboratory kinetic studies have identified several reactions which obey the alkaline hydrolysis mechanism under typical geochemical conditions. Three tracers tested so far are applicable in cool reservoirs (80-100 °C), while two should be useful in hotter systems (up to 200°C).

NOMENCLATURE

A effective heat transfer surface area (m^2)

A_r first order pre-exponential factor (s^{-1})

$A_{r,2}$ second order pre-exponential factor (liter/mol-s)

C concentration of reacting tracer (kg/m^3)

C_i inlet concentration in step-change experiment (kg/m^3)

$C(t)$ concentration response of inert tracer (kg/m^3)

c_p average fluid heat capacity (J/kg-K)

D_{eff} effective dispersivity of a reservoir (m^2/s)

E_a first order activation energy (kJ/mol)

$E_{a,2}$ second order activation energy (kJ/mol)

$E(t)$ residence time distribution function (s^{-1})

ΔH^{o} heat of reaction (kJ/mol)

k first order rate constant (s^{-1})

k_2 second order rate constant (liters/mol-s)]

K equilibrium constant

K_T equilibrium constant at the temperature T

K_{25} equilibrium constant at 25 °C

L fracture length (m)

m_p mass of tracer in pulse (kg)

Pe axial dispersion Peclet number

Q volumetric flow rate of fluid (m^3/s)

R universal gas constant = $8.314 \cdot 10^{-3}$ kJ/mol-K

SUE stress unlocking experiment

t time (s)

T fluid temperature (K)

T_i inlet fluid temperature (K)

T_r initial rock temperature (K)

t_{op} time of operation of a reservoir (s)

U average fluid velocity (m/s)

$\dot{V}$ modal volume (m^3)

$\langle V \rangle$ integral mean volume (m^3)

$w_{1/2}$ width at 1/2 height of a tracer response curve (m^3)

z flow direction in one-dimensional flow model (m)

α thermal diffusivity of rock (m^2/s)

λ_r thermal conductivity of rock (W/m-K)

τ_r reaction time (hr)

[ ] Concentration of ionic species (mol/liter)

ACKNOWLEDGMENTS

We thank the Los Alamos National Laboratory and U.S. Department of Energy for the financial support necessary to perform this work. Robert Potter, Charles Grigsby, and Hugh Murphy contributed many useful ideas during the development of the ideas presented. Lois Gritzo provided analytical chemistry support vital to the completion of the many kinetic experiments which went into the construction of Figure 6.

REFERENCES

1. Robinson, B. A., and Tester, J. W., "Dispersed Fluid Flow in Fractured Reservoirs: An Analysis of Tracer-Determined Residence Time Distributions," submitted to J. Geophys. Res. (1984).

2. McCabe, W. J., Barry, B. J., and Manning, U. R., "Radioactive Tracers in Geothermal Underground Water Flow Studies," Geothermics, 12, 83 (1983).

3. Wagner, O. R., "The Use of Tracers in Diagnosing Interwell Reservoir Heterogeneities -- Field Results," J. Pet. Tech., 29, 1410 (1977).

4. Murphy, H. D., Tester, J. W., Grigsby, C. O., and Potter, R. M., "Energy Extraction from Fractured Geothermal Reservoirs in Low-Permeability Crystalline Granite," J. Geophys. Res., 86(B8) 7145 (1981).

5. Horne, R. N., and Rodriguez, F., "Dispersion in Tracer Flow in Fractured Geothermal Systems," Geophys. Res. Letters, 10, 289 (1983).

6. Zyvoloski, G. A. (ed.), "Evaluation of the Second Hot Dry Rock Geothermal Energy Reservoir: Results of Phase I, Run Segment 5," Rept. LA-8940-HDR, Los Alamos National Laboratory, Los Alamos, NM 87545 (1981).

7. Batchelor, A. S., Personal Communication (1983).

8. Tester, J. W., Bivins, R. L., and Potter, R. M., "Interwell Tracer Analyses of a Hydraulically Fractured Granitic Geothermal Reservoir," Soc. Pet. Eng. J., 22, 537 (1982).

9. Dash, Z. V., Murphy, H. D., and Cremer, G. M. (eds.), "Hot Dry Rock Geothermal Reservoir Testing: 1978-1980," Rept. LA-9080-SR, Los Alamos National Laboratory, Los Alamos, NM 87545 (1981).

10. Nichol, D. A. C., and White, A. A. L., "On the Behavior of a Jointed Geothermal Reservoir," submitted to J. Geophys. Res. (1983).

11. Kirby, A. J., in Comprehensive Chemical Kinetics (C. M. Bamford and C. F. H. Tipper, eds.). Elsevier, New York (1972).

Table 1. Magnitudes of Different Single-Fracture Dispersion Mechanisms

Sources: Horne and Rodriguez (1983), Robinson and Tester (1984)

Mechanism	Peclet Number	Comments
Fracture Roughness	very large	scale of dispersion (fracture aperture) is very small compared to overall length scale (well-bore separation distance)
Matrix Diffusion	very large	large apertures and rapid flow velocities minimize matrix diffusion effects
Taylor Dispersion	$150\text{-}3\times10^{4}$	molecular diffusion coefficient varies strongly with temperature, causing wide range in Pe
Point Source-Point Sink Potential Flow	55	calculated assuming dispersion is caused solely by flow streamlines of different length and velocity
Actual Measured Dispersion in Fractured Geothermal Reservoirs	0.5-5	observed dispersion is much greater than can be explained by flow in a single fracture

Table 2. Summary of Tracer Field Experiments

Fenton Hill Experiments

Date	$\dot{V}$ (m^3)	<V> (m^3)	$w_{1/2}$ (m^3)	$w_{1/2}/\dot{V}$
2/9/78	11.4		18.1	1.59
3/1/78	17.0		40.3	2.3
3/23/78	22.7		62.5	2.75
4/7/78	26.5		70.8	2.67
5/9/80	161	1311	227	1.41
9/3/80	178	1845	323	1.81
12/2/80	187	–	303	1.62
12/12/80	266	2173	479	1.80

Rosemanowes Tracer Experiments (1982-1983)

RH6A	1.42		1.68	1.18
RH12	12.3		7.0	0.57
Fluor-escein #3	2390		4870	2.04

Table 3. Results of Kinetic Experiments

$$A_r = (1.0457 \times 10^{-6}) 10^{pH} A_{r,2}$$

$$E_a = E_{a,2} + 45.8$$

Compound	$A_{r,2}$	$E_{a,2}$	$A_r/10^{pH}$	E_a
Ethyl Acetate	4.79×10^{6}	42.7	5.009	88.5
Ethyl Propionate	4.774×10^{6}	43.8	4.992	89.6
Iso-Pentyl Acetate	5.969×10^{7}	52.6	62.42	98.4
Ethyl Pivalate	1.473×10^{11}	98.3	1.54×10^{5}	144.1
Acetamide	1.519×10^{8}	73.5	1.59×10^{2}	119.3

FIGURE CAPTIONS

Fig. 1 Effective Heat Transfer Surface Area Versus Modal Volume

Fig. 2 Fracture Volume Growth Versus Cumulative Energy Extracted

Fig. 3 Internal Temperature Profiles During Long Term Energy Extraction

Fig. 4 Reactive Tracer Behavior During Long Term Energy Extraction

Fig. 5 Hydroxide Concentration Versus Temperature in a Geofluid

Fig. 6 Reaction Time Versus Temperature for Candidate Reactive Tracers

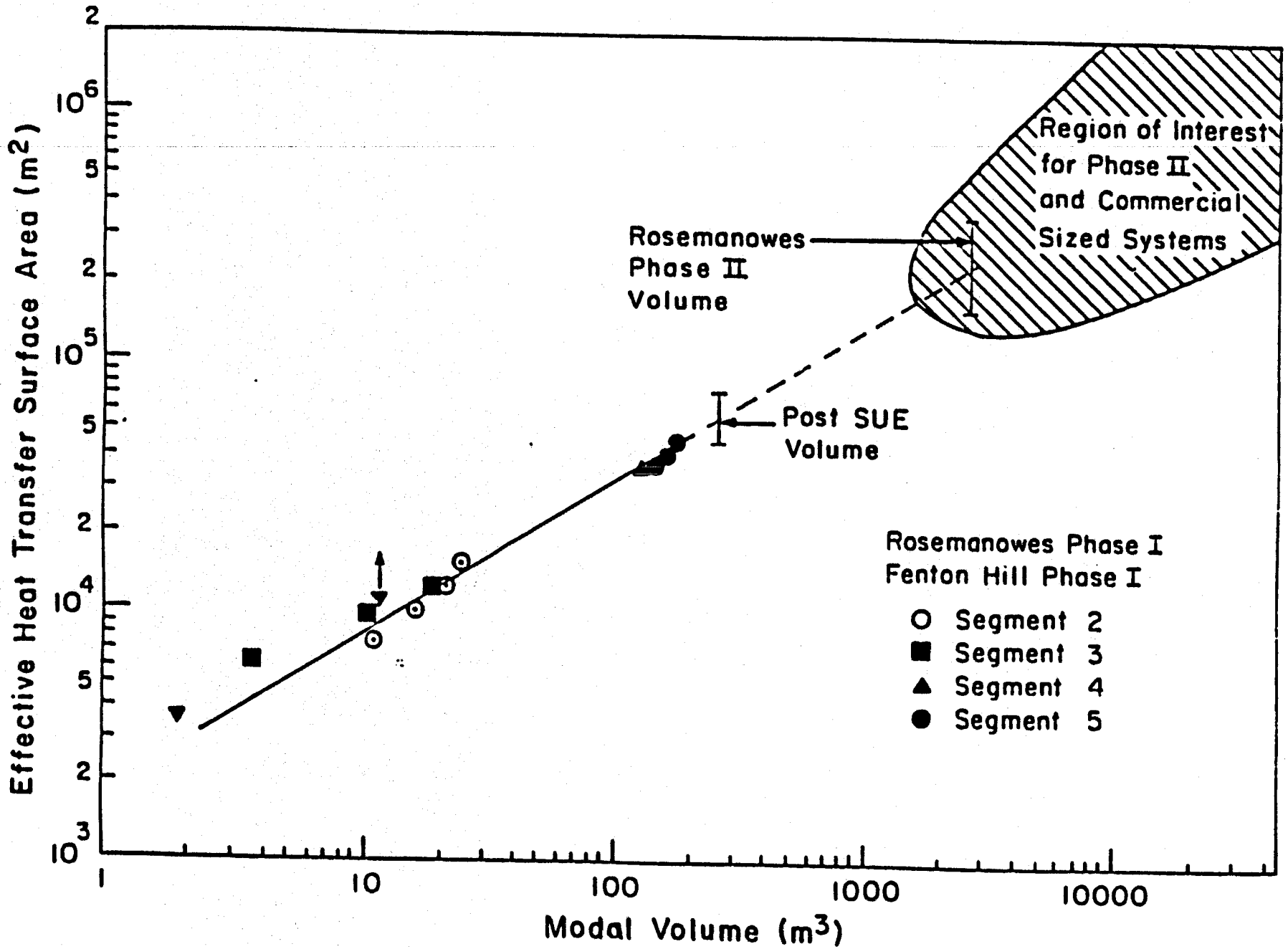
Effective Heat Transfer Surface Area (m^2)
Modal Volume (m^3)
Region of Interest for Phase II and Commercial Sized Systems
Rosemanowes Phase II Volume
Post SUE Volume
Rosemanowes Phase I
Fenton Hill Phase I
Segment 2
Segment 3
Segment 4
Segment 5

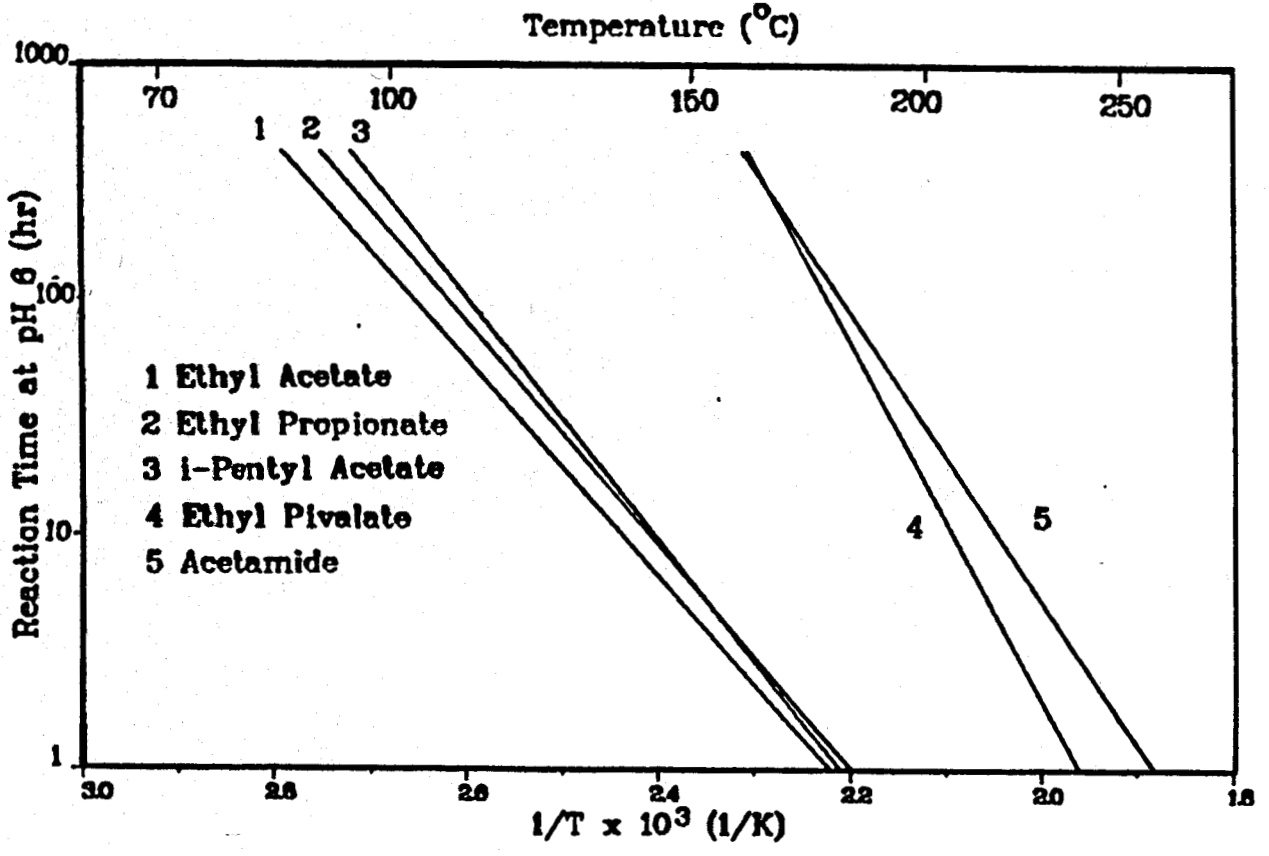
Temperature (°C)
70
100
150
200
250
1000
100
10
1
Reaction Time at pH 6 (hr)
1
2
3
4
5
1 Ethyl Acetate
2 Ethyl Propionate
3 i-Pentyl Acetate
4 Ethyl Pivalate
5 Acetamide
3.0
2.8
2.6
2.4
2.2
2.0
1.8
1/T x 10³ (1/K)

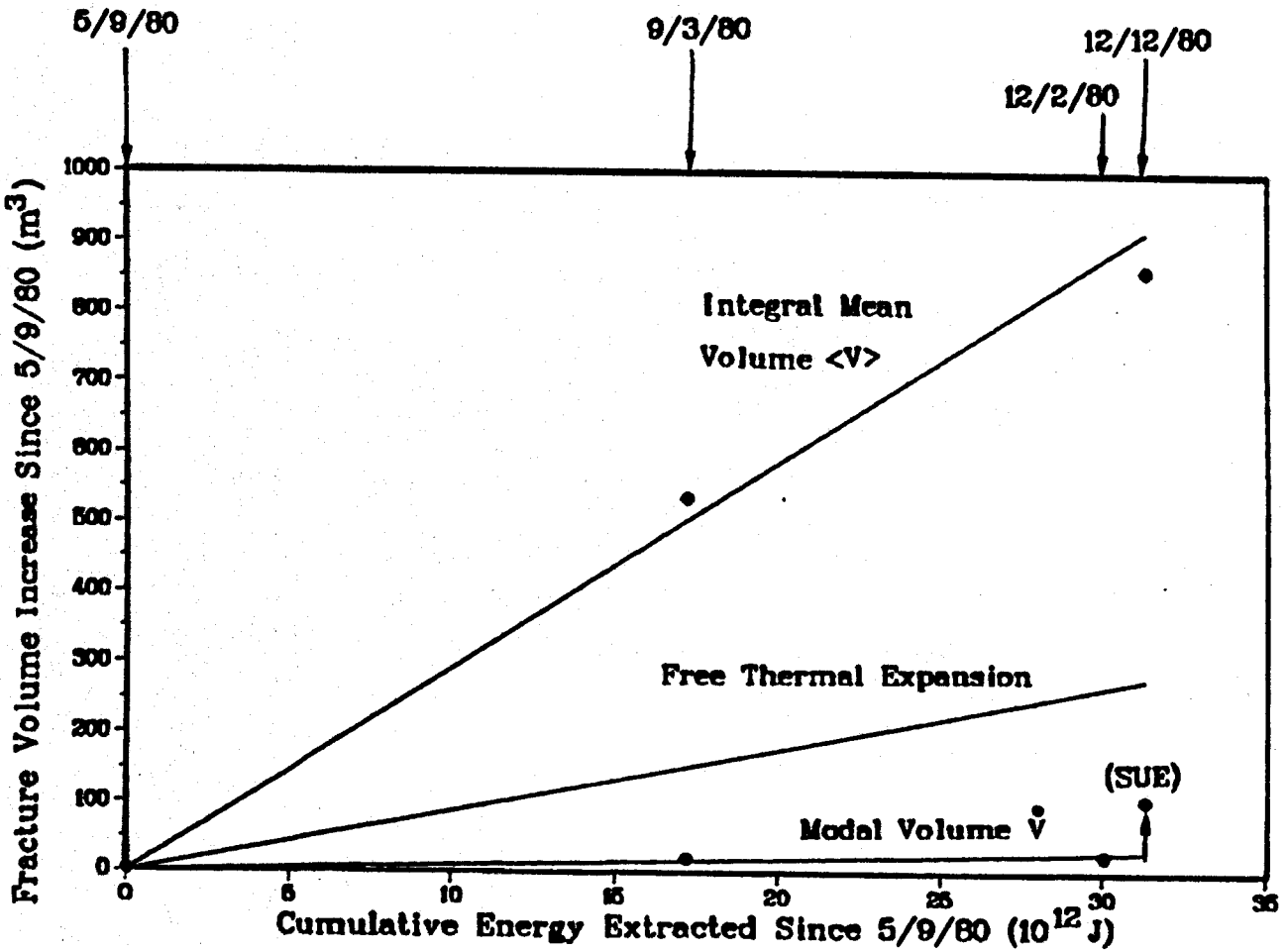
5/9/80
9/3/80
12/12/80
12/2/80
Integral Mean
Volume <V>
Free Thermal Expansion
(SUE)
Modal Volume V̇
Fracture Volume Increase Since 5/9/80 (m3)
Cumulative Energy Extracted Since 5/9/80 (10^12 J)
0
100
200
300
400
500
600
700
800
900
1000
0
5
10
15
20
25
30
35

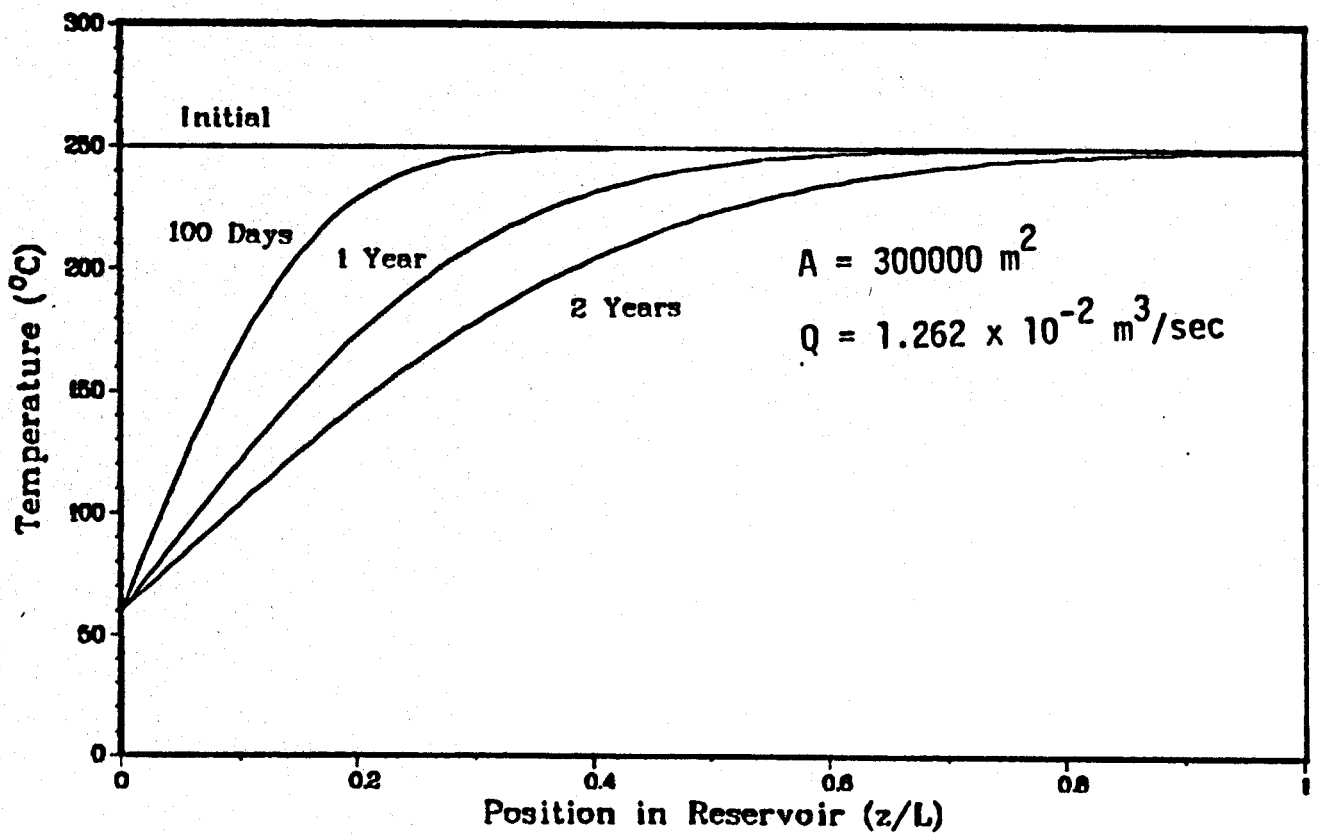
Initial
100 Days
1 Year
2 Years
A = 300000 m2
Q = 1.262 x 10-2 m3/sec
Temperature (°C)
Position in Reservoir (z/L)
300
250
200
150
100
50
0
0
0.2
0.4
0.6
0.8
1

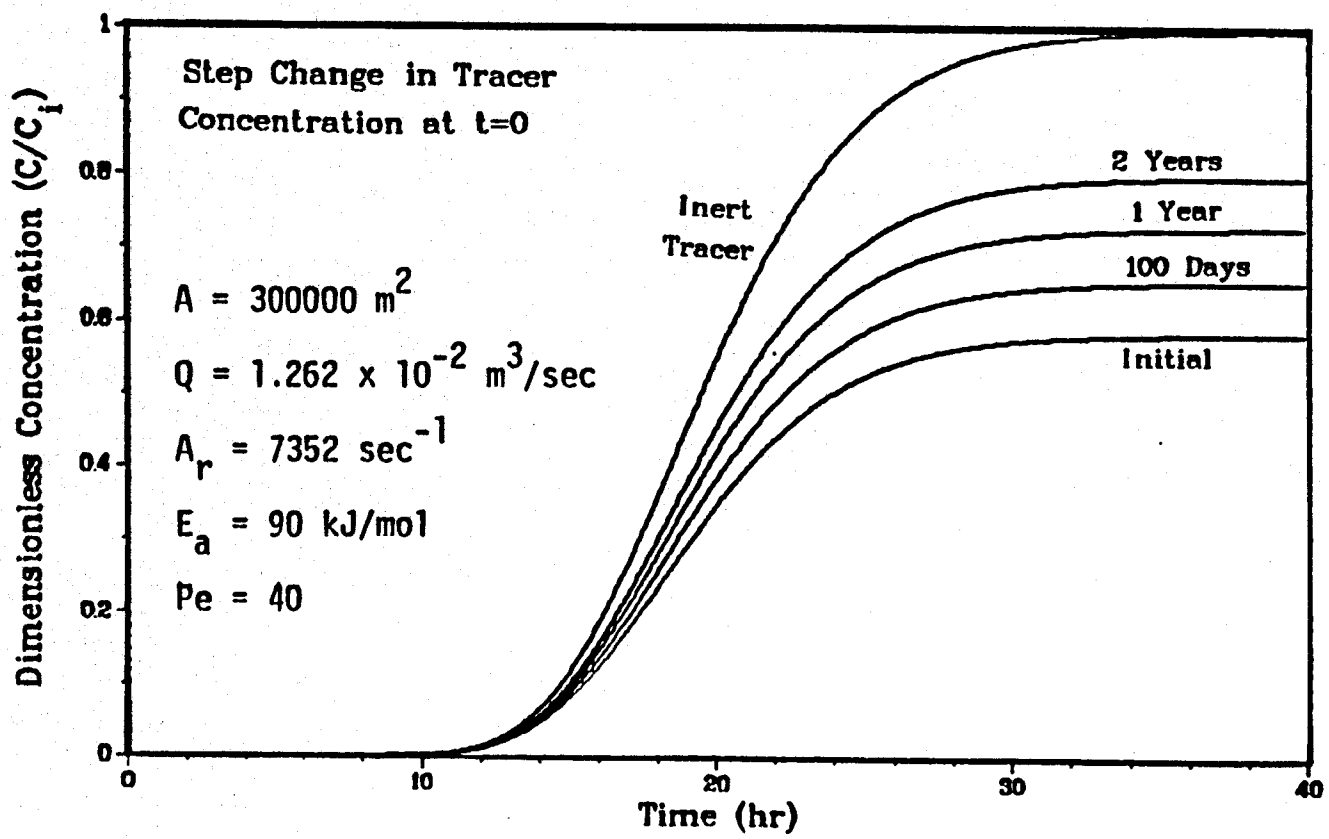
Step Change in Tracer
Concentration at t=0
A = 300000 m2
Q = 1.262 x 10-2 m3/sec
Ar = 7352 sec-1
Ea = 90 kJ/mol
Pe = 40
Inert
Tracer
2 Years
1 Year
100 Days
Initial
Dimensionless Concentration (C/Ci)
Time (hr)
0
0.2
0.4
0.6
0.8
1
0
10
20
30
40

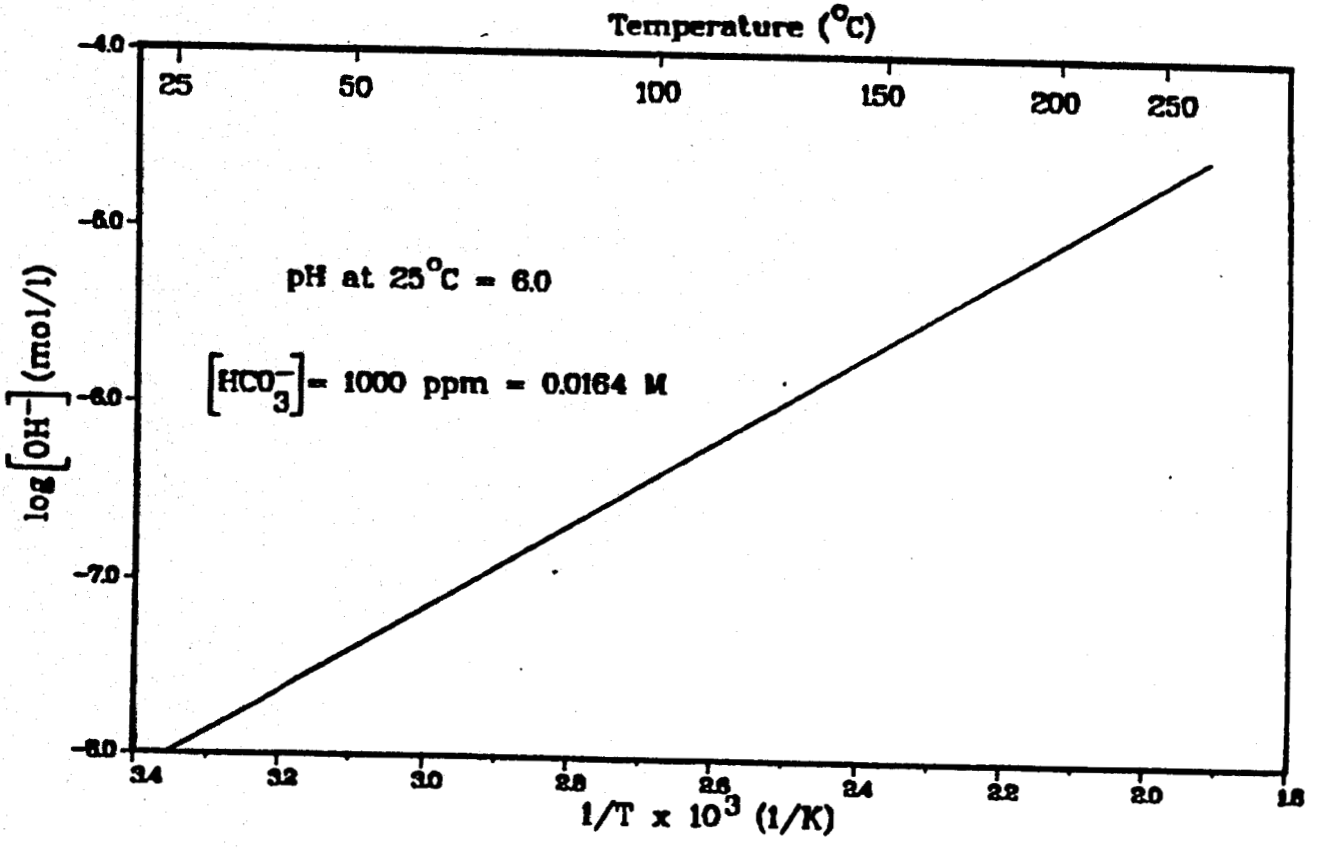
Temperature (°C)
25
50
100
150
200
250
-4.0
-5.0
-6.0
-7.0
-8.0
pH at 25°C = 6.0
[HCO3-] = 1000 ppm = 0.0164 M
log[OH-] (mol/l)
3.4
3.2
3.0
2.8
2.6
2.4
2.2
2.0
1.8
1/T x 10^3 (1/K)